2. J. A. EDWARDS and J. S. DOOLITTLE, Tetrafluoroethylene promoted dropwise condensation, *Int. J. Heat Mass Transfer* **8**, 663 (1965).
3. D. W. BUTCHER and C. W. HONOUR, Tetrafluoroethylene coatings on condenser tubes, *Int. J. Heat Mass Transfer* **9**, 835 (1966).
4. L. TOPPER and E. BAER, Dropwise condensation of vapour and heat transfer rates, *J. Colloid Sci.* **10**, 225 (1955).
5. J. T. DAVIES and Sir ERIC RIDEAL, *Interfacial Phenomena.* Academic Press, London (1961).
6. H. W. FOX and W. A. ZISMAN, The spreading of liquids on low energy surfaces, II. Modified tetrafluoroethylene polymers, *J. Colloid Sci.* **7**, 109 (1952).
7. A. B. PONTER, G. A. DAVIES, W. BEATON and T. K. ROSS, The measurement of contact angles under conditions of heat transfer when a liquid film breaks on a vertical surface, *Int. J. Heat Mass Transfer* **10**, 1633 (1967).
8. J. R. PARTINGTON, *An Advanced Treatise on Physical Chemistry*, Vol. 2. Longmans, London (1955).

Int. J. Heat Mass Transfer. Vol. 11, pp. 377–379. Pergamon Press 1968. Printed in Great Britain

RADIATING, CONVECTING AND CONDUCTING FINS: NUMERICAL AND LINEARIZED SOLUTIONS

E. M. SPARROW† and E. R. NIEWERTH

Coordenação dos Programas Pós-Graduados de Engenharia, Universidade do Brasil, Rio de Janeiro, Brasil

(*Received* 12 *April* 1967 *and in revised form* 21 *August* 1967)

NOMENCLATURE

A, area of fin cross section;
C, circumference of fin cross section;
h, heat-transfer coefficient;
k, thermal conductivity of fin;
L, fin length;
N_{cv}, convection parameter, equation (1a);
N_r, radiation parameter, equation (1a);
Q, rate of heat loss from fin;
T, temperature;
X, dimensionless coordinate, x/L;
x, coordinate measuring axial distance along fin ($x = 0$ is fin base).

Greek symbols
ϵ, emittance of fin surface;
η, fin effectiveness, equation (2);
θ, temperature ratio, T/T_b;
σ, Stefan–Boltzmann constant.

Subscripts
b, fin base;
∞, fluid bulk.

Superscript
$*$, effective radiation environment.

INTRODUCTION

THE PURPOSE of this note is to provide representative results for one-dimensional heat conduction in fins of axially unchanging cross section, the surface heat transfer involving both convection and radiation. The governing energy equation is

$$\mathrm{d}^2\theta/\mathrm{d}X^2 = N_r(\theta^4 - \theta^{*4}) + N_{cv}(\theta - \theta_\infty) \qquad (1)$$

$$\theta = \frac{T}{T_b}, \quad X = \frac{x}{L}, \quad N_r = \frac{\epsilon\sigma T_b^3 CL^2}{kA}, \quad N_{cv} = \frac{hCL^2}{kA},$$

$$\theta^* = \frac{T^*}{T_b}, \quad \theta_\infty = \frac{T_\infty}{T_b} \qquad (1a)$$

in which T_b, T_∞, and T^* are, respectively, the temperatures at the fin base, in the adjacent fluid, and of the effective radiation environment.‡ The area and circumference of the cross section are A and C; while L is the length of the fin. Equation (1) is to be solved subject to the boundary conditions $\theta(0) = 1$ and $(\mathrm{d}\theta/\mathrm{d}X)_1 = 0$, and for specified values of the four independent parameters N_r, N_{cv}, θ^*, and θ_∞.

In addition to direct numerical solutions, linearized

† Present address: Department of Mechanical Engineering, University of Minnesota, Minneapolis, Minnesota, 55455, U.S.A.

‡ The absorbed radiant energy per unit time and area is $\epsilon\sigma T^{*4}$.

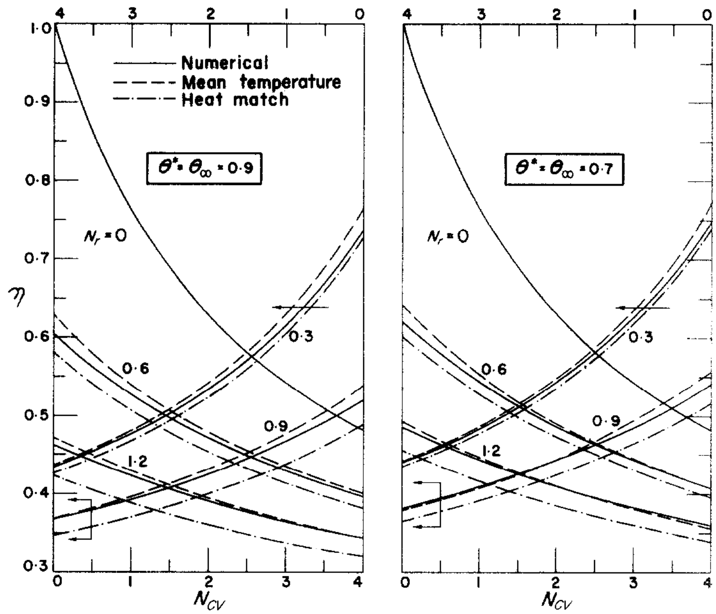

FIG. 1. Effectiveness of convecting and radiating fins, $\theta^* = \theta_\infty = 0{\cdot}9$ and $0{\cdot}7$.

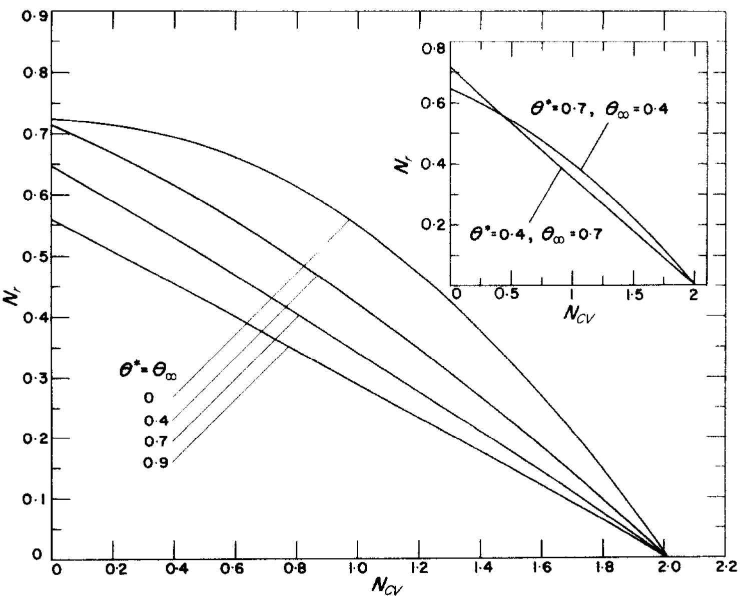

FIG. 2. Relationship between N_{cv} and N_r for optimum operating conditions.

solutions have also been obtained by letting $\theta^4 = \theta\tilde{\theta}^3$, where $\tilde{\theta}$ is independent of x. The linearization constant $\tilde{\theta}$ was determined by two alternative approaches. In the first method (termed the heat match), one uses the linearized solution to evaluate the heat conduction Q_c at the fin base and the overall heat loss Q_l by convection and radiation from the surfaces of the fin, the radiation involving fourth-power emission. For an exact solution, Q_c and Q_l are necessarily equal; for the linearized solution, the condition $Q_c = Q_l$ provides a means for determining $\tilde{\theta}$. In the second method (mean temperature method), $\tilde{\theta}$ is determined as the average of the θ values at $x = 0$ and $x = L$.

The fin heat transfer can be expressed in terms of the effectiveness as

$$\eta = \frac{Q}{Q_{\text{ideal}}} = \frac{-kA(\mathrm{d}T/\mathrm{d}x)_0}{CL[\epsilon\sigma(T_b^4 - T^{*4}) + h(T_b - T_\infty)]} \tag{2}$$

where the ideal fin is one of infinite thermal conductivity.

The presence of four independent parameters coupled with journal space limitations restricts the presentation of results to a few representative cases. Figure 1 shows a plot of fin effectiveness as a function of N_{cv} for parametric values of N_r, with $\theta^* = \theta_\infty = 0{\cdot}9$ and $0{\cdot}7$. The solid lines correspond to the numerical solutions, while the dashed and dot-dashed lines are for the linearized solutions. The uppermost curve ($N_r = 0$) in each graph is for purely convective heat loss, while the ordinate intercepts ($N_{cv} = 0$) correspond to purely radiative heat loss.

For given values of N_r and N_{cv}, the fin effectiveness corresponding to simultaneous radiative and convective loss is seen to be lower than either of the respective η values for purely radiative and purely convective heat loss. Moreover, while η decreases with increasing values of N_r and N_{cv}, as for the respective cases of pure radiation and pure convection, the rate of decrease is markedly influenced by the simultaneous action of the two transport mechanisms. At low N_r (small radiation contribution), η decreases rapidly with N_{cv}. On the other hand, at larger N_r, η is much less sensitive to increases in N_{cv}. Similarly, η becomes less sensitive to N_r when N_{cv} is large. Within the range of the figure, η is not a strong function of the specific values of θ^* and θ_∞.

It is also seen from Fig. 1 that the accuracy of the results based on the mean temperature model is generally very good, being within that required for design.

Consideration is now given to the so-called optimum fin, for which the heat transfer per unit volume of fin is a maximum. The determination of the optimum condition depends on the specifics of the fin cross section. Numerical results will be derived here for the straight fin of rectangular profile (thickness t). If the fin width is fixed, the optimum is found by regarding the profile area A_p ($= Lt$) as a constant and varying either L or t until the maximum heat transfer is encountered. In the numerical determination of the optimal condition, it is especially advantageous to use the linearized models since the relevant partial derivatives can be evaluated from closed form expressions. In view of its relative simplicity, the mean temperature model was employed.

The optimum fin results are shown in Fig. 2. The main portion of the figure corresponds to cases where $\theta^* = \theta_\infty$, while the inset shows a few cases for which $\theta^* \neq \theta_\infty$. The ordinate intercepts are the N_r values defining optimum conditions for purely radiating fins, while the abscissa intercept ($2{\cdot}0142$) is the optimum condition for purely convecting fins.

The figure shows that for simultaneous radiative and convective heat loss, the N_r, N_{cv} values defining the optimum are always less than are those when these processes act separately. In other words, the optimum N_r decreases with increasing N_{cv}, and the optimum N_{cv} decreases with increasing N_r. Once the optimum N_r, N_{cv} are known, then the ratio N_r/N_{cv} yields the corresponding value of $\epsilon\sigma T_b^3/h$. The fin effectivenesses η that correspond to the optimum N_r, N_{cv} of Fig. 2 generally fall in the neighborhood of $0{\cdot}6$.